

LETTER TO THE EDITOR

## A 0.8 mm heterodyne facility receiver for the APEX telescope<sup>★</sup>

C. Risacher<sup>1,2</sup>, V. Vassilev<sup>1</sup>, R. Monje<sup>1</sup>, I. Lapkin<sup>1</sup>, V. Belitsky<sup>1</sup>, A. Pavolotsky<sup>1</sup>, M. Pantaleev<sup>1</sup>, P. Bergman<sup>2,1</sup>, S.-E. Ferm<sup>1</sup>, E. Sundin<sup>1</sup>, M. Svensson<sup>1</sup>, M. Fredrixon<sup>1</sup>, D. Meledin<sup>1</sup>, L.-G. Gunnarsson<sup>1</sup>, M. Hagström<sup>1</sup>, L.-Å. Johansson<sup>1</sup>, M. Olberg<sup>1</sup>, R. Booth<sup>1</sup>, H. Olofsson<sup>1</sup>, and L.-Å. Nyman<sup>2</sup>

<sup>1</sup> Onsala Space Observatory, Chalmers University of Technology, 43992, Sweden  
e-mail: [crisache@eso.org](mailto:crisache@eso.org)

<sup>2</sup> European Southern Observatory, Casilla 19001, Santiago 19, Chile

Received 6 April 2006 / Accepted 24 April 2006

### ABSTRACT

**Aims.** The new APEX telescope, located on Llano Chajnantor in Northern Chile, will have high resolution spectroscopic instruments covering the wavelength region from 0.20 to 1.30 mm (210–1500 GHz).

**Methods.** In May 2005, the first facility receiver for the band 0.79–1.07 mm (279–381 GHz) was installed together with backends providing down to 60 kHz spectral resolution. This instrument that operates in double sideband mode uses superconducting tunnel junctions (SIS) as mixing elements operating at 4 K to achieve close to quantum-limited noise performances. The receiver is cooled by a closed-cycle cooling machine that allows continuous operation. The receiver design minimizes moving parts and is fully operated by remote to improve its reliability and the ease of use.

**Results.** The double sideband (DSB) receiver temperatures are in the range 50–70 K, which typically results in a DSB system noise temperature of about 100 K in excellent weather conditions and between 100–200 K in good weather conditions.

**Key words.** submillimeter – instrumentation: detectors – techniques: spectroscopic

## 1. Introduction

The APEX 12 m telescope is installed in the Atacama Desert in Northern Chile in one of the best sites for submillimeter astronomy. The telescope is described in Güsten et al. (2006). It has a Cassegrain cabin and two Nasmyth cabins that accommodate a variety of millimeter and sub-millimeter bolometric and spectroscopic instruments. The Nasmyth cabin A contains the facility's heterodyne instrument and allows installation of two more instruments, one of them currently being the First Light Facility Submillimeter (Flash) receiver, a two-channel 460/810 GHz spectroscopic instrument (Heyminck et al. 2006). The Onsala Space Observatory is responsible for the delivery of the facility heterodyne receivers, for the bands 210–275 GHz, 275–370 GHz, 385–500 GHz, and 1.25–1.39 THz, all located in a single cryostat. The first receiver (for the 2nd band) was installed in May 2005 and its performance is described here.

## 2. Instrument design

### 2.1. General description

A schematic of the receiver in the telescope with the location of the various components of the system is shown in Fig. 1. Before reaching the instrument detector, the signal beam goes through a system of 11 mirrors: the main dish, the sub-reflector, 4 mirrors

in the Cassegrain cabin, and 5 mirrors in the Nasmyth cabin A. The telescope focus is near the vertex of the primary dish. The optics were designed to provide frequency-independent illumination of the secondary for every partial receiver band. The first mirror after the Nasmyth flange M 7 rotates around the elevation axis in order to select different instruments placed in cabin A. The next mirror, M 8, rotates to select between the different receiver bands of the cryostat. The last 2 mirrors are placed inside the cryostat (Fig. 2)

The intermediate frequency (IF) band of the receiver is 4–8 GHz. The IF output is fed into a common IF module, with a total power detector detecting the whole 4 GHz signal, which is then used for the continuum observations. The common IF selects a 1 GHz band inside the 4–8 GHz band, usually centered at 6 GHz, and then amplifies and downconverts it to the 0–1 GHz band before going to the backends. The backend is a fast Fourier transform spectrometer (FFTS) described in Klein et al. (2006) having up to 16 384 channels with a separation of 61 kHz.

### 2.2. Receiver design

The heterodyne receiver is based on a superconducting-insulator-superconducting (SIS) junction mixer that needs to be operated at a temperature around 4 K. The cooling machine is a hybrid closed-cycle system using a Gifford Mac-Mahon 2-stage refrigerator, together with a Joule-Thomson refrigerator. The 2-stage cooling gives a temperature of about 70 K and 15 K for the outer shields. The Joule-Thomson circuitry cools the helium gas further down to about 4.2 K, where the most sensitive components, the mixer and the IF low noise amplifier, are placed (Fig. 2).

<sup>★</sup> APEX, the Atacama Pathfinder Experiment, is a collaboration between the Max-Planck-Institut für Radioastronomie (MPIfR) at 50%, Onsala Space Observatory (OSO) at 23%, and the European Southern Observatory (ESO) at 27% to construct and operate a modified ALMA prototype antenna as a single dish on the high-altitude site of Llano Chajnantor.

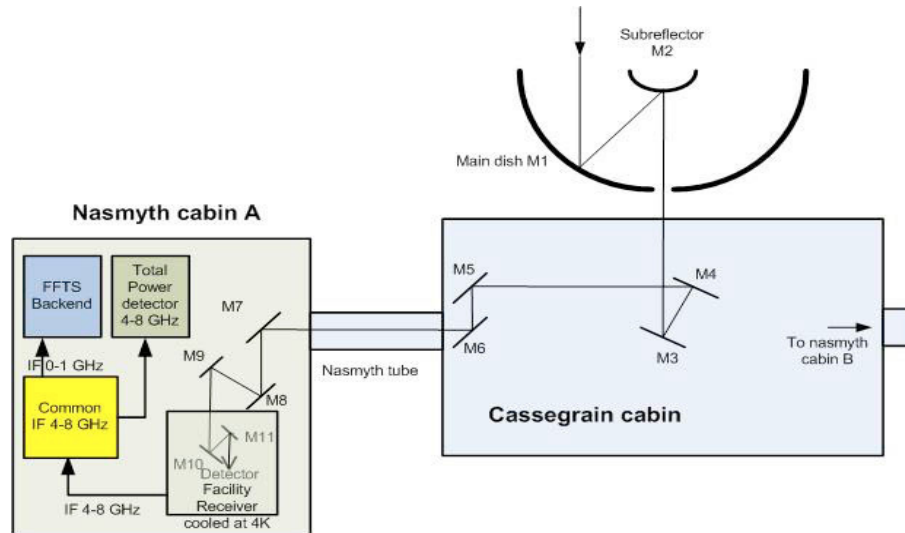


**Fig. 1.** General layout. The signal passes 11 mirrors before reaching the detector. The receiver IF output then goes to a common IF module where part of it is detected by a total power detector used for the continuum observations, and the rest is down-converted to the 0–1 GHz band before going to the backends.

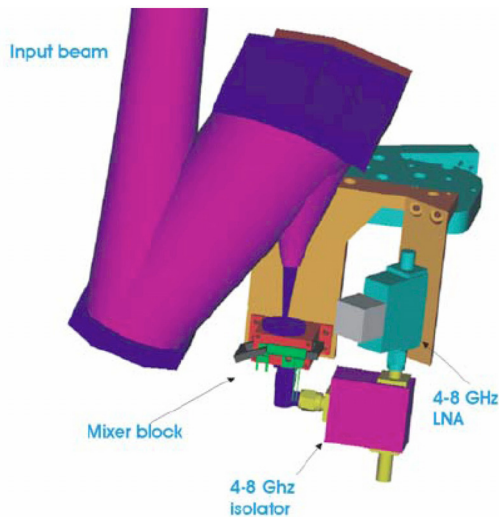


**Fig. 2.** View of the inner part of the cryostat. The input beam is shown. The mixer, IF isolator, and IF amplifier are on the 4 K cold plate.

The local oscillator (LO) is a Carlstrom Gunn oscillator for the frequency range 95–125 GHz followed by a Virginia Diodes tunerless tripler. The LO signal is injected via an external beam splitter consisting of a 12  $\mu\text{m}$  Mylar film. The receiver RF operating range is 279–381 GHz limited only by the local oscillator. The mixer itself has a broader bandwidth (260–385 GHz). There are two cryogenic low noise amplifiers providing about 40 dB amplification of the 4–8 GHz IF signal.

The receiver is entirely remotely operated and has very few mechanical tuners. Since the mixer is completely tunerless, there are no moving parts inside the cryostat. The Gunn oscillator has two moving motors for tuning the frequency and power optimization, whereas the tripler is tunerless. The tuning of the receiver takes less than 5 min. The mixer operation is double side-band (DSB), meaning that the signal and image band appear equally at the IF. Table 1 summarizes the main characteristics of the system and a complete description of the receiver can be found in Risacher (2005).

**Table 1.** Receiver system summary.

Frequency range	279–381 GHz
Receiver noise temperature (DSB)	50–70 K
Receiver cooling	Closed-cycle at 4 K
System noise temperature (DSB)	100–200 K (typical)
Intermediate frequency	4–8 GHz

### 3. Laboratory results

When tested in the laboratory, the receiver noise temperatures were about 30–50 K across the band when measured directly at the output of the receiver. This represents about 2–3 times the quantum noise,  $h\nu/k$ . These measurements were performed in a test cryostat with liquid helium. With the closed-cycle machine, the noise performance was similar. The total power stability measurements gave an Allan time between 5–10 s with a 600 MHz integration bandwidth, and the spectroscopic Allan time was between 20–100 s with a 1 MHz integration bandwidth.

### 4. On-site results

#### 4.1. Noise performance

The receiver was installed on the telescope in May 2005 and its commissioning took place during subsequent months. Figure 3 shows the measured noise temperatures across the frequency band between May and December 2005. The set of data represented by triangles (lower curve) is the receiver noise temperature when measured directly at the output of the receiver, while the rectangular points (middle curve) represent the receiver temperatures during observations. These receiver noise temperatures include the whole IF chain and the backend (FFTS), adding about 15–20 K. The diamond shaped points (upper curve) show typical system temperatures in various weather conditions. During the best weather conditions (precipitable water vapor PWV below 0.5 mm), the DSB system temperature is as low as 100 K across the band. In good weather (PWV between 0.5 and 1 mm), the system temperature is between 100–200 K.

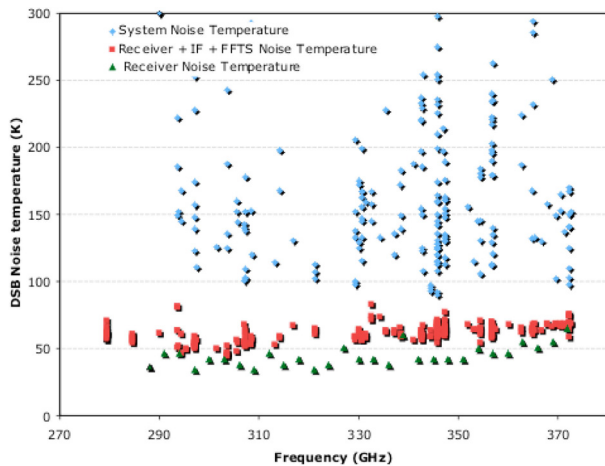


**Fig. 3.** Typical receiver and system temperatures measured throughout the observing season in May–December 2005.

#### 4.2. Receiver limitations

In the closed-cycle cooling machine, the cold head movement creates 1 Hz mechanical vibrations. The LO coupling to the receiver is influenced directly, causing the receiver gain to vary with the vibrations. Therefore, a  $\sim 400$  MHz standing wave often appears in the baselines. This ripple, while having little impact on narrow line observations, precluded any work on weak and broad extragalactic lines in 2005. To minimize this variation, the local oscillator power was adjusted to a very low value to decrease the mixer conversion gain thereby reducing its sensitivity to these modulations. This in turn degraded the receiver noise slightly. Moreover, an optimized tuning procedure was developed in early 2006. It was found that by slightly changing the tuning frequency ( $<150$  MHz offset), it is always possible to find a stable tuning with little or no ripple.

During 2005, there was also a problem around the  $\text{CO}(J = 3 \rightarrow 2)$  frequency, where lines observed alternatively in upper sideband (USB) and lower sideband (LSB) showed different intensities. This was very likely due to a resonance in the mixer, causing lines in the USB tuning to be miscalibrated. The mixer was replaced in February 2006 and the new mixer, with equally good noise performance, does not show this problem.

Finally, it was discovered in December 2005 that the LO system can produce a second line at  $7/6$  times the frequency of observation, which might pump the mixer enough to produce a very weak additional mixing. This phenomenon was observed on at least one occasion at the low-frequency edge of the receiver and is under investigation.

#### 4.3. Continuum observations

For continuum pointings, the full IF bandwidth of the receiver is used, i.e. 4 GHz for each sideband, hence 8 GHz. Figure 4 shows two pointing scans (in the elevation and the azimuthal directions, respectively) toward Uranus at a frequency of 350/338 GHz. Each continuous scan had a length of  $180''$  and took about 30 s. At the time of the observations (July 11, 2005) the diameter of Uranus was  $3.6''$ , so the fitted widths reflect the full half-power beam width (FHPBW) at 350/338 GHz. A more complete coverage of the beam shape can be obtained by using the on-the-fly (OTF) mapping technique. An OTF map of Mars taken on 2005-11-12, observed at 345/357 GHz with  $4 + 4$  GHz bandwidth, produced a circular source where the level of the

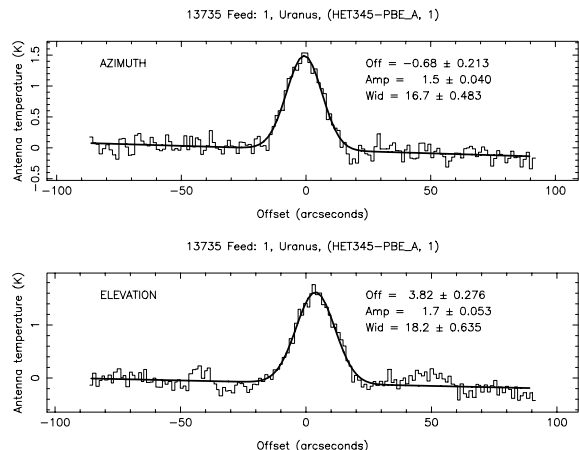


**Fig. 4.** Cross-scan pointing on Uranus.

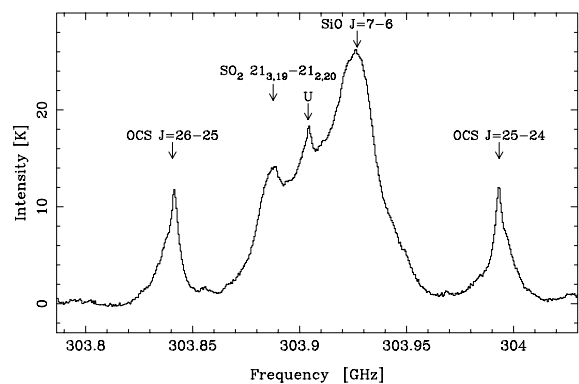


**Fig. 5.** Example of OCS measurement in Orion-KL. The rotational transitions  $J = 25 \rightarrow 24$  and  $J = 26 \rightarrow 25$  from different sidebands appear quite close in the final IF spectrum with similar line intensities. Note that the asymmetry of the  $J = 26 \rightarrow 25$  line (coming from the USB around 316 GHz) is opposite that of the  $J = 25 \rightarrow 24$  line.

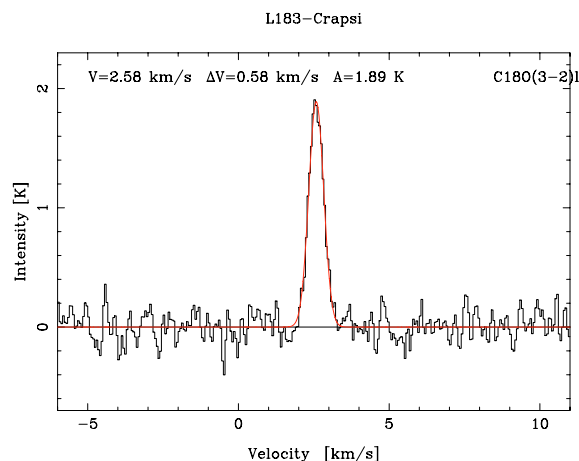


**Fig. 6.**  $\text{C}^{18}\text{O}(J = 3 \rightarrow 2)$  spectrum of the cold dark cloud L183.

side-lobes were below the  $-24$  dB level. From that measurement, the beam size at 345 GHz was estimated to be  $18''$ , consistent with the Rayleigh criterion.

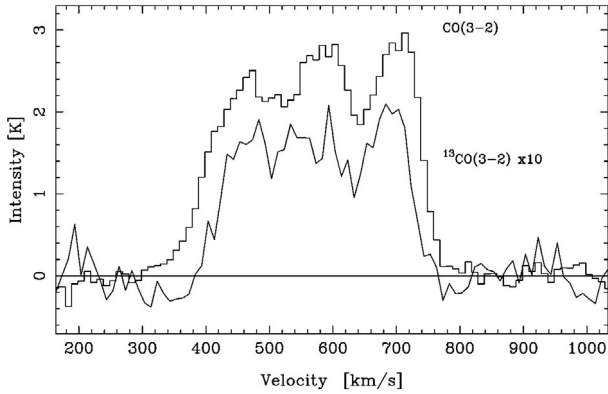


**Fig. 7.** CO( $J = 3 \rightarrow 2$ ) and  $^{13}\text{CO}(J = 3 \rightarrow 2)$  in NGC 4945 at the velocity resolution of  $10 \text{ km s}^{-1}$ . Note that these data were taken in March 2006 with the new mixer using the optimized-tuning procedure.

#### 4.4. Spectroscopic observations

For the spectroscopic observations presented here, the IF bandwidth was limited to 1 GHz by the FFTS backend bandwidth, and the line intensities are in the  $T_a^*$  scale.

The receiver is double sideband; therefore, each of the sidebands will contribute to the final spectrum with a given gain, which may be frequency-dependent along the mixer tuning range. Sideband ratios of the receiver can be estimated by observing high  $J$  rotational transitions of OCS. This molecule is ideal in our case, because the spacing between adjacent rotational transitions is about 12 GHz, the same as the separation between the signal and image bands. The line intensities of these high  $J$  transitions should be almost equal. These lines are easily detected in sources like Orion KL (cf. Schilke et al. 1997). Figure 5 shows a spectrum of Orion KL taken at 304/316 GHz with the OCS  $J = 25 \rightarrow 24$  and  $J = 26 \rightarrow 25$  transitions in the signal and image band respectively. Results from 6 different

tunings toward Orion KL tend to show that the sideband ratio is close to 1.0 for the different frequencies tested. Depending on line blending and calibration, the accuracy of this method is estimated to be about 15%.

As an example of other spectroscopic measurements, Fig. 6 shows a  $\text{C}^{18}\text{O}(J = 3 \rightarrow 2)$  spectrum of the cold dark cloud L183, which was previously observed by Crapsi et al. (2005), in  $\text{C}^{18}\text{O}(J = 2 \rightarrow 1)$  with the IRAM 30 m telescope. The center velocity and line width agree perfectly with their data. As an example of extragalactic measurement, Fig. 7 shows broad (about  $400 \text{ km s}^{-1}$  wide) lines of CO( $J = 3 \rightarrow 2$ ) and  $^{13}\text{CO}(J = 3 \rightarrow 2)$  in NGC 4945. The NGC 4945 data shown here from March 2006 agree quite well with SEST observations (cf. Mauersberger et al. 1996; Curran et al. 2001) given the differences in resolution and beam efficiencies.

This receiver (together with a small optical telescope) is also used to construct pointing models of the telescope. Its high sensitivity makes it possible to easily detect a large number of circumstellar envelopes in the CO( $J = 3 \rightarrow 2$ ) line (whose compact emission is ideal for this purpose), resulting in very good sky coverage.

*Acknowledgements.* This work is part of the APEX Project and is funded by the Swedish Research Council and the Wallenberg Foundation by their respective grants. Part of this work was supported by research grant via EU FP6 AMSTAR Program.

#### References

- Crapsi, A., Caselli, P., Walmsley, C. M., et al. 2005, *ApJ*, 619, 379
- Curran, S. J., Johansson, L. E. B., Bergman, P., Heikkilä, A., & Aalto, S. 2001, *A&A*, 367, 457
- Güsten, R., Nyman, L. Å., Schilke, P., et al. 2006, *A&A*, 454, L13
- Heyminck, S., et al. 2006, *A&A*, 454, L21
- Klein, B., et al. 2006, *A&A*, 454, L29
- Mauersberger, R., Henkel, C., Whiteoak, J. B., Chin, Y.-N., & Tieftrunk, A. R. 1996, *A&A*, 309, 705
- Risacher, C. 2005, Ph.D. Thesis, Chalmers University
- Schilke, P., Groesbeck, T. D., Blake, G. A., & Phillips, T. G. 1997, *ApJS*, 108, 301